Inorg. Chem. **2005**, *44*, 3121–3126

Salt-Inclusion Synthesis of Two New Polar Solids, $Ba_6Mn_4Si_{12}O_{34}Cl_3$ and $Ba_6Fe_5Si_{11}O_{34}Cl_3$

Xunhua Mo, Erin Ferguson, and Shiou-Jyh Hwu*

Department of Chemistry, Clemson University, Clemson, South Carolina 29634-0973

Received February 14, 2005

A new family of salt-containing, mixed-metal silicates (CU-14), $Ba_6Mn_4Si_{12}O_{34}Cl_3$ (**1**) and $Ba_6Fe_5Si_{11}O_{34}Cl_3$ (**2**), was synthesized via the $BaCl_2$ salt-inclusion reaction. These compounds crystallize in the noncentrosymmetric (NCS) space group $Pmc2_1$ (No. 26), adopting 1 of the 10 NCS polar, nonchiral crystal classes, *mm*2 (C_{2v}). The cell dimensions are $a = 6.821(1)$ Å, $b = 9.620(2)$ Å, $c = 13.172(3)$ Å, and $V = 864.4(3)$ Å^3 for **1** and $a = 6.878(1)$ Å, $b = 9.664(2)$ Å, $c = 13.098(3)$ Å, and $V = 870.6(3)$ Å^3 for **2**. The structures form a composite framework made of the $(M_{4+x}Si_{12-x}O_{34})^{9-}$ (M = Mn, $x = 0$; M = Fe, $x = 1$) covalent oxide and $(Ba_6Cl_3)^{9+}$ ionic chloride sublattices. The covalent framework exhibits a pseudo-one-dimensional channel where the extended barium chloride lattice $(Ba_3Cl_{1.5})_\infty$ resides, and it consists of fused eight-membered meta-silicate rings propagating along [100] via sharing two opposite $[Si_2O_7]^{6-}$ units to form an acentric lattice. Single-crystal structure studies also reveal the $ClBa_4$ unit adopting an interesting seesaw configuration, in which the lone pair electrons of chlorine preferentially face the oxide anions of the transition metal silicate channel, thus forming the observed polar frameworks. Similar to the synthesis of organic–inorganic hybrid materials, the salt-inclusion method facilitates a promising approach for the directed synthesis of special framework solids, including NCS compounds, via composite lattices.

Introduction

Design and synthesis of noncentrosymmetric (NCS) materials have attracted constant attention due to their potential materials applications, such as chiral catalysis, ferroelectricity, and nonlinear optics.[1] Some recent synthesis strategies for NCS inorganic solids include using chiral organic molecules or metal complexes as templating agents,[2] employing enantiopure metal−organic clusters as secondary building blocks,[3] acentric packing of helical chains via directed metal−ligand−metal linkages,[4] incorporating acentric polyanions to stereochemically enforce acentricity of the bulk,[5] and incorporating cations with nonbonding electron pairs or d^0 transition metal cations showing cooperative second-order, Jahn−Teller (SOJT) distortions.[6]

* Author to whom correspondence should be addressed. E-mail: shwu@clemson.edu.

(1) (a) Bein, T. *Curr. Opin. Solid State Mater. Sci.* **1999**, *4*, 85−96. (b) Keszler, D. A. *Curr. Opin. Solid State Mater. Sci.* **1999**, *4*, 155−162. (c) Yaghi, O. M.; Li, H.; Davis, C.; Richardson, D.; Groy, T. L. *Acc. Chem. Res.* **1998**, *31*, 474−484. (d) Marder, S. R.; Sohn, J. E.; Stucky, G. D. *Materials for Nonlinear Optics: Chemical Perspective*; ACS Symposium Series 455; American Chemical Society: Washington, DC, 1991.

(2) (a) Che, S.; Liu, Z.; Ohsuna, T.; Sakamoto, K.; Terasaki, O.; Tatsumi, T. *Nature* **2004**, *429*, 281−284. (b) Bu, X.; Zheng, N.; Li, Y.; Feng, P. *J. Am. Chem. Soc.* **2003**, *125*, 6024−6025. (c) Lin, C.-H.; Wang, S.-L. *Chem. Mater.* **2002**, *14*, 96−102. (d) Yu, J.; Wang, Y.; Shi, Z,; Xu, R. *Chem. Mater.* **2001**, *13*, 2972−2978. (e) Bruce, D.; Wilkinson, A. P.; White, M. G.; Bertrand, J. A. *J. Solid. State. Chem.* **1996**, *125*, 228−233. (f) Bruce, D.; Wilkinson, A. P.; White, M. G.; Bertrand, J. A. *J. Chem. Soc., Chem. Commun.* **1995**, 2059−2060.

(3) (a) Seitz, M.; Kaiser, A.; Stepfhuber, S.; Zabel, M.; Reiser, O. *J. Am. Chem. Soc.* **2004**, *126*, 11426−11427. (b) Anokhina, E. V.; Jacobson, A. J. *J. Am. Chem. Soc.* **2004**, *126*, 3044−3045. (c) Kesanli, B.; Lin, W. *Coord. Chem. Rev.* **2003**, *246*, 305−326. (d) Evans, O. R.; Lin, W. *Chem. Mater.* **2001**, *13*, 3009−3017. (e) Seo, J. S.; Whang, D.; Lee, H.; Jun, S.; Oh, J.; Jeon, Y.; Kim, K. *Nature* **2000**, *404*, 982−986. (f) Kepert, C. J.; Prior, T. J.; Rosseinsky, M. J. *J. Am. Chem. Soc.* **2000**, *122*, 5158−5168.

(4) (a) Maggard, P. A.; Kopf, A. L.; Stern, C.; Poeppelmeier, K. R. *CrystEngComm* **2004**, *6*, 451−457. (b) Maggard, P. A.; Stern, C. L.; Poeppelmeier, K. R. *J. Am. Chem. Soc.* **2001**, *123*, 7742−7743. (c) Maggard, P. A.; Kopf, A. L.; Stern, C. L.; Poeppelmeier, K. R.; Ok, K. M.; Halasyamani, P. S. *Inorg. Chem.* **2002**, *41*, 4852−4858.

(5) (a) Norquist, A. J.; Heier, K. R.; Halasyamani, P. S.; Stern, C. L.; Poeppelmeier, K. R. *Inorg. Chem.* **2001**, *40*, 2015−2019. (b) Sykora, R. E.; Ok, K. M.; Halasyamani, P. S.; Albrecht-Schmitt, T. E. *J. Am. Chem. Soc.* **2002**, *124*, 1951−1957.

(6) (a) Ok, K. M.; Halasyamani, P. S. *Angew. Chem., Int. Ed.* **2004**, *43*, 5489−5491. (b) Shehee, T. C.; Sykora, R. E.; Ok, K. M.; Halasyamani, P. S.; Albrecht-Schmitt, T. E. *Inorg. Chem.* **2003**, *42*, 457−462. (c) Goodey, J.; Broussard, J.; Halasyamani, P. S. *Chem. Mater.* **2002**, *14*, 3174−3180. (d) Porter, Y.; Bhuvanesh, N. S. P.; Halasyamani, P. S. *Inorg. Chem.* **2001**, *40*, 1172−1175. (e) Porter, Y.; Ok, K. M.; Bhuvanesh, N. S. P.; Halasyamani, P. S. *Chem. Mater.* **2001**, *13*, 1910−1915. (f) Halasyamani, P. S.; O'Hare, D. *Chem. Mater.* **1998**, *10*, 646−649. (g) Halasyamani, P. S.; O'Hare, D. *Inorg. Chem.* **1997**, *36*, 6409−6412.

10.1021/ic050228t CCC: $30.25
Published on Web 04/06/2005

Our continued investigation of salt-inclusion solids sheds new light on the exploration of special frameworks via composite (hybrid) solids of mixed ionic and covalent sublattices, e.g., $CuPO_4 \cdot BaCl$,[7a] $ANbAsO_5Cl$ (A = Rb, Cs),[7b] $A_2M_3(X_2O_7)_2 \cdot$salt (A = K, Rb, Cs; M = Mn, Cu, X = P, As) (CU-2),[7c] $Na_2Cs_2Cu_3(P_2O_7)_2Cl_2$ (CU-4),[7d] $Na_5ACu_4(AsO_4)_4Cl_2$ (A = Rb, Cs),[7e,f] $Cs_2Cu_7(P_2O_7)_4 \cdot 6CsCl$ (CU-9), $Cs_2Cu_5(P_2O_7)_3 \cdot 3CsCl$ (CU-11),[7g,h] and $Ba_2Mn(Si_2O_7)Cl$ (CU-13).[7i] The NCS compounds discovered thus far in the salt-inclusion systems (CU-9, CU-11, and CU-13) share a common feature in that the incorporated salt lattices are made of chlorine-centered acentric secondary building units (SBU), ClA_4M_2 (A/M = Cs/Cu, Ba/Mn), thus the polar framework.[7g−i] It should be noted, however, the incorporation of an acentric SBU is a necessary but not sufficient condition alone to accomplish bulk acentricity. As expected, the materials can crystallize such that the distortions occur in an antiparallel manner, thus producing bulk centricity. Meanwhile, it is worth noting that the formation of the polar salt-inclusion compound $Ba_2MnSi_2O_7Cl$ (CU-13) demonstrates a cooperative effect attributed to the combined utilities of the polar $Si_2O_7^{6-}$ anion and the Jahn−Teller Mn^{3+} d^4 cation.

During our continued exploration of NCS solids via salt-inclusion synthesis, we discovered two isostructural polar solids, $Ba_6Mn_4Si_{12}O_{34}Cl_3$ (**1**) and $Ba_6Fe_5Si_{11}O_{34}Cl_3$ (**2**), that contain transition metal cations. These new compounds exhibit a pseudo-one-dimensional channel structure in which a fascinating extended salt lattice consisting of chlorine-centered SBU, $ClBa_4$, is recognized. Unlike previously discovered CU series,[7] the nonbonding electron pairs of the chloride anions, instead of coordinating to transition metal centers, preferentially face the oxide anions of the transition metal silicate channel, thus allowing the formation of the observed polar frameworks. In this report, we once again demonstrate the utility of salt inclusion in the synthesis of special framework solids, particularly the NCS compounds.

Experimental Section

Synthesis. Crystals of **1** and **2** were grown by employing the eutectic $BaCl_2$/NaCl flux (with the charge-to-flux ratio 1:3 by weight) in a fused silica ampule. The reactants were ground and loaded in a nitrogen-blanketed drybox and then sealed under vacuum prior to heating.

1 was first crystallized in the molten salt medium from the reaction containing Na_2O (3 mmol, Aldrich, 85%), MnO (3 mmol, Aldrich, 99.99%), GeO_2 (4 mmol, Aldrich, 99.99%), and CsCl (3 mmol, ICN, 99.9%). The mixture was heated to 850 °C at 2 °C/min and isothermed for 3 days, followed by slow cooling to room temperature. A low yield (ca. 10%) of reddish needlelike crystals of $Ba_6Mn_4Si_{12}O_{34}Cl_3$ was isolated after washing off the salt with deionized water. The incorporation of silicon was likely due to the interaction of silica ampule with molten salt, and the major products were $BaGe_2O_5$ (ca. 30%) and $MnGeO_3$ (60%) according to the single-crystal X-ray indexing. High-yield (ca. 90%) synthesis was then attempted by heating the stoichiometric mixture of $BaO/BaCl_2/Mn_2O_3/MnO/SiO_2$ at 1000 °C for 6 days in a sealed quartz ampule.

Yellowish column crystals of **2** (90% yield) were grown by introducing the mixture of BaO (4.5 mmol, Aldrich, 97%), $BaCl_2$ (1.5 mmol, Aldrich, 99.9%), Fe_2O_3 (2.5 mmol, Alfa, 99.99%), and SiO_2 (11 mmol, Aldrich, fused, 99.9%) into the eutectic $BaCl_2$/NaCl flux. The reaction conditions were the same as those employed above. High-yield (ca. 90%) synthesis can also be carried out in a sealed quartz ampule using the stoichiometric mixture of $BaO/BaCl_2/Fe_2O_3/SiO_2$ at 1000 °C for 6 days.

Crystallographic Studies. Single-crystal structures were determined by X-ray diffraction methods. Data collection was carried out on a four-circle Rigaku AFC8 diffractometer equipped with a Mercury CCD area detector with Mo Kα (λ = 0.710 73 Å) radiation and T = 293 K. The structures were solved by direct methods using the SHELXTL-6.1 program and refined on F^2 by least-squares, full-matrix techniques.[8] PLATON ADDSYM analysis[9] of the structures of **1** and **2** did not reveal any additional symmetry elements and confirmed the NCS group $Pmc2_1$. The Flack parameters converged at 0.04(4) and 0.32(2), respectively.[10] The latter indicates the possibility of the existence of an inversion twin. Cl(1) was refined as a partially occupied site,[11] while Cl(2) was solved as two split sites. In this report, the average position of these split Cl(2)/Cl(3) sites was used for clarity in the structure illustration. In **2**, Si(3) was refined as the mixed Si(3)/Fe(3) site, which gives rise to the refined formula $Ba_6Fe_{4+x}Si_{12-x}O_{34}Cl_3$ (x = 1). As indicated in Table 1, **1** and **2** crystallize in 1 of the 10 NCS polar, nonchiral crystal classes, *mm*2 (C_{2v}).[12] The subsequent investigation of **2** shows an equivalent second-harmonic-generation (SHG) response as that of SiO_2. Table 2 lists the atomic parameters for **1**.

X-ray Photoemission Spectroscopy. XPS was employed to investigate the oxidation state of Fe cations in **2**. The preliminary XPS data collections of selected crystals were carried out using the EM facilities at Clemson University,[13] and high-resolution core line scans at Iowa State University.[14] The high-resolution Fe(2p) scans are shown in Figure 1, where four sets of data were presented with respect to different sample pretreatments.

(7) (a) Etheredge, K. M. S.; Hwu, S.-J. *Inorg. Chem.* **1995**, *34*, 3123−3125. (b) Ulutagay, M.; Shimek, G. L.; Hwu, S.-J.; Taye, H. *Inorg. Chem.* **1998**, *37*, 1507−1512. (c) Huang, Q.; Ulutagay, M.; Michener, P. A.; Hwu, S.-J. *J. Am. Chem. Soc.* **1999**, *121*, 10323−10326. (d) Huang, Q.; Hwu, S.-J.; Mo, X. *Angew. Chem., Int. Ed. Engl.* **2001**, *40*, 1690−1693. (e) Hwu, S.-J.; Ulutagay-Kartin, M.; Clayhold, J. A.; Mackay, R.; Wardojo, T. A.; O'Connor, C. J.; Krawiec, M. *J. Am. Chem. Soc.* **2002**, *124*, 12404−12405. (f) Clayhold, J. A.; Ulutagay-Kartin, M.; Hwu, S.-J.; Koo, H.-J.; Whangboo, M.-H.; Voigt, A.; Eaiprasertsak, K. *Phys. Rev. B* **2002**, *66*, 052403. (g) Huang, Q.; Hwu, S.-J. *Inorg. Chem.* **2003**, *42*, 655−657. (h) Huang, Q.; Ulutagay-Kartin, M.; Mo, X.; Hwu, S.-J. *Mater. Res. Soc. Symp. Proc.* **2003**, *755*, DD12.4. (i) Mo, X.; Hwu, S.-J. *Inorg. Chem.* **2003**, *42*, 3978−3980.

(8) (a) Sheldrick, G. M. In *Crystallographic Computing 3*; Sheldrick, G. M., Kruger, C., Goddard, R., Eds.; Oxford University Press: London, 1985; pp 175−189. (b) Sheldrick, G. M. *SHELXTL, Version 6.1 Structure Determination Software Programs*; Bruker Analytical X-ray Systems Inc.: Madison, WI, 2001.

(9) (a) Spek, A. L. *J. Appl. Crystallogr.* **2003**, *36*, 7−13. (b) Spek, A. L. *PLATON. A Multipurpose Crystallographic Tool*; Utrecht University: Utrecht, The Netherlands, 2005. http://www.Cryst.Chem.uu.nl./PLATON.

(10) (a) Flack, H. D.; Bernardinelli, G. *J. Appl. Crystallogr.* **2000**, *33*, 1143−1148. (b) Flack, H. D.; Bernardinelli, G. *Acta Crystallogr.* **1999**, *A55*, 908−915. (c) Flack, H. D. *Acta Crystallogr.* **1983**, *A39*, 876−881.

(11) Crystallographically, the half-occupied Cl(1) site could be refined as a full O, in turn, leading to different oxidation states of $Fe^{3.0+}$ or $Fe^{3.5+}$, respectively. The XPS experiments and stoichiometric synthesis confirmed the presence of the oxidation state of Fe^{3+}. The site was ultimately refined as a partially occupied Cl in both structures. In **2**, in addition, the refinement of occupancy was in constraint with that of Fe(3), a mixed site with Si(3); see text.

(12) Halasyamani, P. S.; Poeppelmeier, K. R. *Chem. Mater.* **1998**, *10*, 2753−2769.

Table 1. Crystallographic Data for **1** and **2**

param	**1**	**2**
empirical formula	$Ba_6Mn_4Si_{12}O_{34}Cl_3$	$Ba_6Fe_5Si_{11}O_{34}Cl_3$
fw	2031.23	2062.63
space group, Z	$Pmc2_1$ (No. 26), 1	$Pmc2_1$ (No. 26), 1
T, °C	25	25
a, Å	6.821(1)	6.878(1)
b, Å	9.620(2)	9.664(2)
c, Å	13.172(3)	13.098(3)
V, Å^3	864.4(3)	870.6(3)
μ(Mo Kα), mm^{-1}	8.894	9.407
D_{calc}, g cm^{-3}	3.902	3.934
data/restraints/params	1936/1/158	2195/1/173
Flack param	0.04(4)	0.32(2)
R1/wR2/GOF[a] (all data)	0.0474/0.0906/1.002	0.0270/0.0567/1.07

[a] $R1 = \Sigma||F_o| - |F_c||/\Sigma|F_o|$. $wR2 = \{[\Sigma[w(F_o^2 - F_c^2)^2]/\Sigma[w(F_o^2)^2]\}^{1/2}$; $w = 1/[\sigma^2(F_o^2) + (0.0407P)^2 + 10.3635P]$ for **1** and $w = 1/[\sigma^2(F_o^2) + (0.0177P)^2 + 5.3028P]$ for **2**, where $P = (F_o^2 + 2F_c^2)/3$.

Table 2. Atomic Coordinates and Equivalent Displacement Parameters for $Ba_6Mn_4Si_{12}O_{34}Cl_3$ (**1**)

atom	Wyckoff notatn/sof	x	y	z	U_{iso} (Å^2)[a]
Ba(1)	2a	0	0.64346(9)	0.02471(7)	0.0172(2)
Ba(2)	2b	0.5	0.9724(1)	0.07799(8)	0.0272(3)
Ba(3)	2b	0.5	0.5096(1)	−0.2452(1)	0.0378(4)
Mn(1)	2a	0	0.0190(2)	−0.0146(2)	0.0167(5)
Mn(2)	2a	0	0.3689(2)	0.2092(2)	0.0118(5)
Si(1)	4c	−0.2689(4)	0.8429(3)	−0.1703(2)	0.0121(6)
Si(2)	4c	−0.7326(4)	0.3011(3)	0.0141(2)	0.0132(6)
Si(3)	2a	0	0.3291(4)	−0.1634(3)	0.0107(8)
Si(4)	2a	0	0.0482(4)	−0.2737(3)	0.0106(8)
O(1)	4c	−0.800(1)	0.1433(7)	0.0240(7)	0.024(1)
O(2)	2b	−0.5	0.838(2)	−0.195(2)	0.061(5)
O(3)	2a	0	0.887(1)	0.1159(9)	0.029(3)
O(4)	4c	−0.193(1)	0.9500(9)	−0.2577(6)	0.033(2)
O(5)	2a	0	0.159(1)	−0.1792(8)	0.011(2)
O(6)	4c	−0.200(2)	0.8925(9)	−0.0633(6)	0.044(3)
O(7)	4c	−0.201(2)	0.6883(9)	−0.1929(9)	0.054(3)
O(8)	2a	0	0.414(1)	−0.2650(8)	0.021(2)
O(9)	2b	−0.5	0.301(1)	0.008(1)	0.052(5)
O(10)	4c	−0.798(1)	0.3978(9)	0.1070(7)	0.036(2)
O(11)	4c	−0.813(2)	0.3688(8)	−0.0921(7)	0.040(3)
Cl(1)	2b/0.5	0.5	0.198(1)	−0.2314(8)	0.034(2)
Cl(2)	2b/0.34(4)	0.5	0.678(2)	0.086(2)	0.035(5)
Cl(3)	2b/0.66(4)	0.5	0.644(1)	0.022(1)	0.042(5)

[a] Equivalent isotropic U defined as one-third of the trace of the orthogonalized $\mathbf{U}_{ij}$ tensor.

The core line scans of etched samples show two sets of Fe(2p) peaks around 707/720 and 711/725 eV, while unetched samples only have two peaks around 711/725 eV. The binding energies for metallic Fe 2p 3/2 and 1/2 are 707/720 eV, so it appears that the sample was reduced by the etching process. In any event, the high-resolution XPS Fe core line spectroscopy, as expected, is sensitive to the different oxidation states, and the resulting spectra qualitatively indicate that the oxidation state of iron is Fe^{3+}.

UV−Vis Diffuse Reflectance Spectroscopy. The spectra of **1** and **2**, as shown in Figure 2, were acquired according to the reported procedures.[15] The absorptions above 3.5 eV are due to ligand-to-metal charge transfer from the SiO_4^{4-} oxyanion. The absorption bands at the energy region lower than 3.2 eV are attributed to the d−d transitions of the incorporated transition metals.[16]

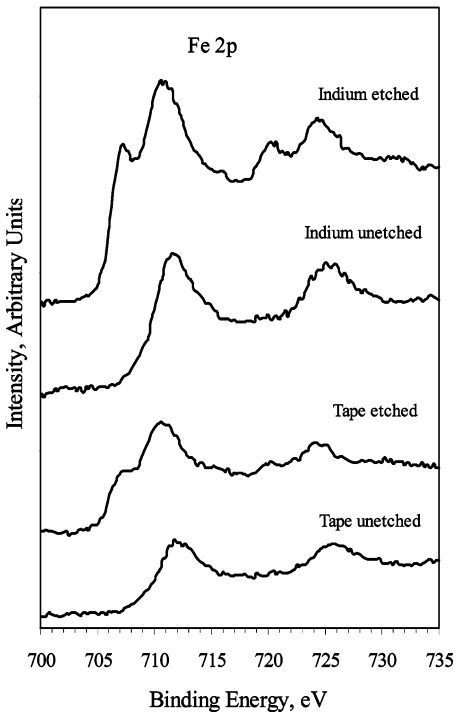

Figure 1. High-resolution Fe(2p) core line photoelectron spectra of the $Ba_6Fe_5Si_{11}O_{34}Cl_3$ samples with different mounting methods (on indium and tape) and pretreatment conditions (etched and unetched).

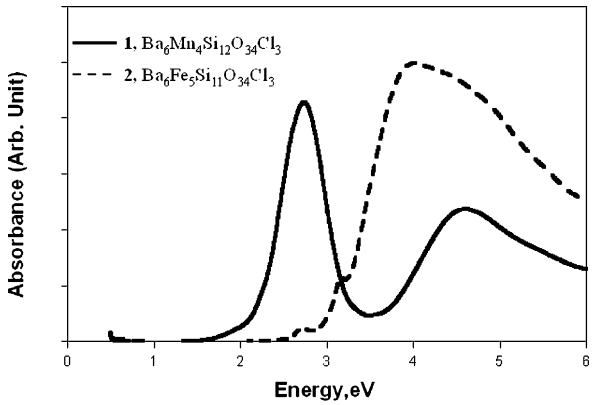

Figure 2. UV−vis diffuse reflectance spectra of **1** and **2**.

Results and Discussion

Systematic investigation for the possible solid solution series $Ba_6M_{4+x}Si_{12-x}O_{34}Cl_3$ (M = Mn, Fe; $x = 0-1$) suggested that **1** and **2** are point compounds. The Mn analogue of **2**, $Ba_6Mn_5Si_{11}O_{34}Cl_3$, where the extra 1 mol of Mn^{3+} cations would reside in the Si(3) tetrahedral site (see below), evidently could not be synthesized. This can possibly be attributed to the thermodynamic factor where the gain of octahedral field stabilization energy cannot be manifested

(13) The XPS spectra were obtained on a KRATOS AXIS 165 spectrometer equipped with monochromatized aluminum anode (15 keV, 15 mA). The working pressure of analysis chamber was 8×10^{-9} Torr. Survey scans for the sample were run with an analyzer pass energy of 80 eV and for component scans of Fe 2p and Si 2p at 20 eV. The selected pale yellow columns of **2** were evenly spread on carbon tape. The binding energy was corrected by the background adventitious C 1s binding energy of 284.8 eV. Each scan was smoothed 3 times with Kenel width 1 using the quadratic Savitzk−Golay method. The raw spectra were fitted with the processing program after automatically subtracting the background.

(14) Smith, M. D.; Miller, G. J. *Inorg. Chem*. **2003**, *42*, 4165−4170.

(15) Ulutagay-Kartin, M.;.Hwu, S.-J.; Clayhold, J. A. *Inorg. Chem.* **2003**, *42*, 2405−2409.

(16) Lever, A. B. P. *Inorganic Electronic Spectroscopy*, 2nd ed; Elsevier Science Publishers BV: New York, 1984.

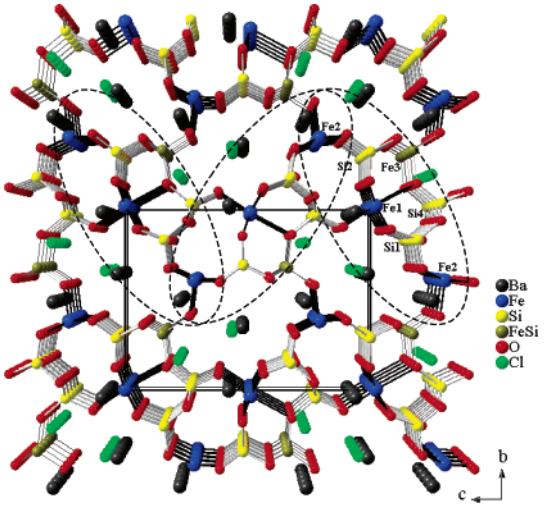

Figure 3. Perspective structure of **2** showing the connectivity of the asymmetric units (outlined by dotted circles) and eight-ring channels. See text. The color code of circles is the same throughout the report.

unless the Mn^{3+} d^4 cation resides in octahedral and related sites. Aliovalent cation substitution necessary for the synthesis of the proposed $Ba_6Mn_5Si_{11}O_{34}Cl_3$ does not impose thermodynamic incentive, thus the absence of the Mn analogue. It is unclear, however, why the Fe analogue of **1**, $Ba_6Fe_4Si_{12}O_{34}Cl_3$, does not exist either. We suspect that the phase compatibility is in favor of the formation of **2** at the given temperature region.

The crystal structure of **2** (Figure 3) represents the general features observed in the three-dimensional framework of the CU-14 family. The asymmetric Fe−O−Si units (outlined by dotted circles) propagate along the polar axis, i.e., the 2_1-screw axis along *c*. Upon viewing along the *a* axis, one can also see that the extended framework consists of oval-shaped 8-ring channels, in which the new barium chloride lattice resides.

One notable difference between **1** and **2** is that the latter contains disordered Si^{4+}/Fe^{3+} sites. In **2**, one of the four silicon sites is statistically occupied by iron, e.g., Fe(3) in Figure 3, and their occupancy factor was fixed at 0.5 to give rise to the composition corresponding to an average oxidation state Fe^{3+}. This is consistent with the XPS analysis in which the characteristic spectrum of Fe(III) shows Fe 2p 3/2 and 1/2 at 711.5 and 725.25 eV, respectively, and a shake-up peak at 719.0 eV.[17] The bond distance of Si(3)/Fe(3) to oxygen atoms is ca. 1.73 Å, which is comparable with those found in reported iron silicate compounds that also contain disordered Si and Fe sites.[18] The oxidation states of Mn^{2+}/Mn^{3+} in **1** and Fe^{3+} in **2** are also verified by the bond valence sum (BVS) calculations.[19] The BVS of Mn(1) and Mn(2) in **1** are 2.74 and 3.07; the BVS of Fe(1) and Fe(2) in **2** are 2.97 and 3.02, respectively. Otherwise, the structures with respect to the transition metal oxide and silicate units are normal **(**see the selected bond distances in Table 3).

Table 3. Selected Bond Distances (Å) for **1** and **2**[a]

	$Ba_6Mn_4Si_{12}O_{34}Cl_3$ (**1**)		
	$Mn(1)O_6$		
$Mn(1)-O(1)^{i}$	1.885(8) (2×)	$Mn(1)-O(5)$	2.566(7)
$Mn(1)-O(6)^{ii}$	1.937(5) (2×)	$Mn(1)-O(3)^{iii}$	2.14(1)
	$Mn(2)O_5$		
$Mn(2)-O(7)^{iv}$	1.96(1) (2×)	$Mn(2)-O(8)^{i}$	2.11(1)
$Mn(2)-O(10)^{i}$	1.947(9) (2×)		
	$Si(1)O_4$		
$Si(1)-O(6)$	1.560(9)	$Si(1)-O(2)$	1.610(5)
$Si(1)-O(7)$	1.59(1)	$Si(1)-O(4)$	1.629(8)
	$Si(2)O_4$		
$Si(2)-O(9)$	1.589(3)	$Si(2)-O(10)$	1.600(9)
$Si(2)-O(1)$	1.591(7)	$Si(2)-O(11)$	1.638(9)
	$Si(3)O_4$		
$Si(3)-O(8)$	1.57(1)	$Si(3)-O(5)^{v}$	1.65(1)
$Si(3)-O(11)$	1.626(8) (2×)		
	$Si(4)O_4$		
$Si(4)-O(5)$	1.64(1)	$Si(4)-O(3)$	1.58(1)
$Si(4)-O(4)^{iii}$	1.636(8) (2×)		
	$Ba_6Fe_5Si_{11}O_{34}Cl_3$ (**2**)		
	$Fe(1)O_6$		
$Fe(1)-O(6)^{vi}$	2.004(4) (2×)	$Fe(1)-O(5)$	2.467(7)
$Fe(1)-O(1)^{vii}$	1.922(4) (2×)	$Fe(1)-O(3)$	2.022(6)
	$Fe(2)O_5$		
$Fe(2)-O(10)^{viii}$	1.929(5) (2×)	$Fe(2)-O(8)^{ix}$	1.906(6)
$Fe(2)-O(7)^{x}$	1.985(5) (2×)		
	$Si(1)O_4$		
$Si(1)-O(2)^{i}$	1.602(2)	$Si(1)-O(6)$	1.573(4)
$Si(1)-O(7)$	1.603(5)	$Si(1)-O(4)$	1.628(5)
	$Si(2)O_4$		
$Si(2)-O(9)^{i}$	1.580(2)	$Si(2)-O(10)$	1.582(5)
$Si(2)-O(11)$	1.623(6)	$Si(2)-O(1)$	1.600(4)
	$Si(Fe)(3)O_4$		
$Fe(3)-O(8)$	1.684(6)	$Fe(3)-O(11)$	1.736(7) (2×)
$Fe(3)-O(5)^{xi}$	1.754(6)		
	$Si(4)O_4$		
$Si(4)-O(5)$	1.644(6)	$Si(4)-O(4)$	1.628(5) (2×)
$Si(4)-O(3)^{xi}$	1.571(6)		

[a] Symmetry codes: (i) $-x-1, y, z$; (ii) $-x, y-1, z$; (iii) $x, y-1, z$; (iv) $-x, -y+1, z+1/2$; (v) $x-1, y, z$; (vi) $-x, y, z$; (vii) $1+x, y, z$; (viii) $-1-x, -1+y, z$; $-1-x, y, z$; (ix) $-1-x, 2-y, 0.5+z$; $1+x, -1+y, z$; (x) $x, 1-y, 0.5+z$; (xi) $-1-x, y, z$; (xi) $-1+x, y, z$.

One of the novel features of the CU-14 structure is the formation of the fused eight-membered meta-silicate ring. This condensed ring is acentric, and the Si-centered tetrahedra are linked in the sequence of Si(2)−Si/Fe(3)−Si(4)−Si(1) (Figure 4) via sharing vertex oxygen atoms in the asymmetric unit. Each ring is symmetrical with respect to the mirror symmetry parallel to the (100) plane, through O(2) and O(9) (Figure 4, top). By sharing the opposite $[Si_2O_7]^{6-}$ units made of the Si(3)- and Si(4)-centered tetrahedra, the eight-membered meta-silicate rings are fused and propagate along [100] (Figure 4, bottom). It is noted that the acentric $[Si_2O_7]^{6-}$ units are pointing along $[01\bar{1}]$, thus forming the polar meta-silicate ring.

(17) (a) McIntyre, N. S.; Zetaruk, D. G. *Anal. Chem.* **1977,** *49* (11), 1521−1529. (b) Fujimori, A.; Saeki, M.; Kimizuka, N.; Taniguchi, M.; Suga, S. *Phys. Rev. B* **1986**, *34* (10), 7318−7328. (c) Mekki, A.; Holland, D.; McConville, C. F.; Salim, M. *J. Non-Cryst. Solids* **1996**, *208*, 267−276.

(18) (a) Brunton, G. D.; Harris, L. A.; Kopp, O. C. *Am. Mineral.* **1972**, *57*, 1720−1728. (b) Grey, I. E.; Hoskins, B. F.; Madsen, I. C. *J. Solid State Chem.* **1990**, *85*, 202−219. (c) Bell, A. M. T.; Henderson, C. M. B. *Acta Crystallogr.* **1994**, *C50*, 1531−1536.

(19) (a) Brown, I. D.; Altermatt, D. *Acta Crystallogr.* **1985**, *B41*, 244−247. (b) Brese, N. E.; O'Keeffe, M. *Acta Crystallogr.* **1991**, *B47*, 192−197.

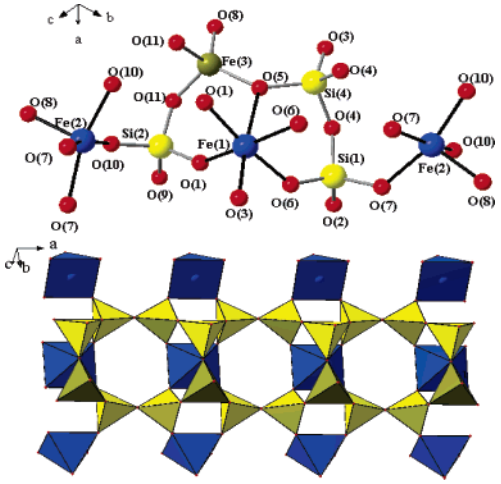

Figure 4. Top: Connectivity of the Fe−O−Si asymmetric unit. Bottom: Polyhedral drawing showing the fused eight-membered, meta-silicate rings and their connectivity with the distorted FeO_5 and FeO_6 polyhedra. See text.

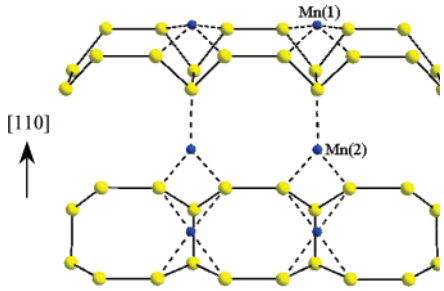

Figure 5. Connectivity of two sheets of fused eight-membered meta-silicate rings. For clarity, only transition metal (blue) and silicon (yellow) cations are shown.

The fused meta-silicate rings are bridged through the distorted $M(1)O_6$ octahedra and $M(2)O_5$ square pyramids centered by M = Mn and Fe. As shown by the skeletal drawing of **1** (Figure 5), the manganese centers of the oxide polyhedra link the fused silicon rings to form a three-dimensional, mixed-metal network. It should be noted that the neighboring sheets of fused rings are related by the *c*-glide mirror plane perpendicular to the *b* axis as well as the 2_1-screw axis along *c* through which a net polarity of the lattice can be preserved.

As shown in Figure 6, it is fascinating to realize that the mixed-metal network consists of pseudo-one-dimensional channel structures where the extended barium chloride lattice resides. The general formula of these composite lattice can be rewritten as $[Ba_6Cl_3][M_{4+x}Si_{12-x}O_{34}]$. The salt lattice forms an acentric structure, see the detailed description below, and is arranged in a preferred orientation to result in the observed polar bulk structure. If one looks into the pseudo-one-dimensional channel, it reveals a gap between the projected salt lattice and the wall of the mixed-metal network. Presumably, the lone-pair electrons of Cl(2) are pointing into this empty space around the proximity of the oxide anions (not shown for clarity). In the structures of **1** and **2**, the shortest nonbonding Cl···O distances are 3.18 and 3.24 Å, respectively.

Also, the novel extended barium chloride salt lattice is made of condensed seesaw units propagating along the *a* axis (Figure 7), and the structural formula can be written as $(Ba_3Cl_{1.5})_\infty$. The overall acentricity of the seesaw structure is therefore preserved.

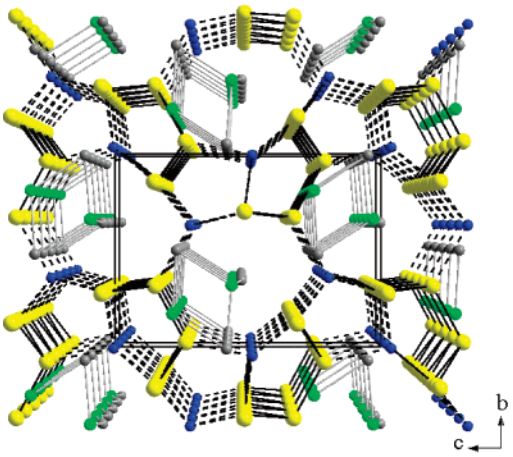

Figure 6. Perspective view of the mixed-metal network structure showing pseudo-one-dimensional channels where the extended Ba−Cl salt lattice resides. Barium atoms are drawn in dark gray, and chlorides, in green circles.

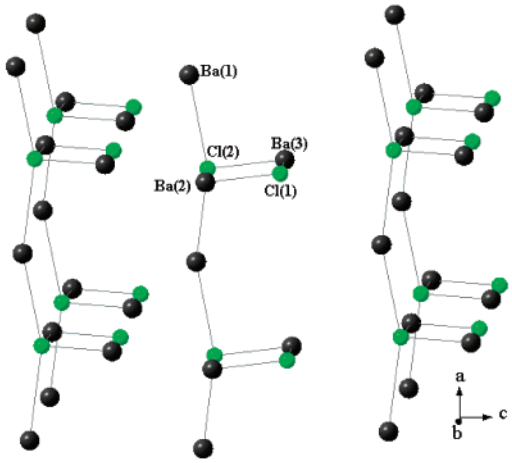

Figure 7. Partial structure of the $(Ba_3Cl_{1.5})_\infty$ chains showing the acentric lattice arrangement. The Cl(1) site is partially occupied. The distances are Cl(1)−Ba(2) = 3.072(9) Å, Cl(1)−Ba(3) = 3.10(1) Å, Cl(2)−Ba(1) = 3.4399(7) Å, Cl(2)−Ba(2) = 2.926(6) Å, and Cl(2)−Ba(3) = 2.936(9) Å.

Unlike the previously reported CU-*n* series (*n* = 2,[7c] 4,[7d] 9, 11[7g]), the Cl^- anion in CU-14 possesses no bonding interaction with the transition metal cations of the covalent framework. Also, compared to other CU phases that contain monovalent chloride salt, neither ion-exchange nor removal of the divalent salt, barium chloride in this case, is possible under the conditions reported previously.[7c] This is likely attributed to the strong electrostatic interaction at the interface of two chemically dissimilar lattices judging from the short Ba−O distances, 2.64−3.70 Å for **1** and 2.68−3.67 Å for **2**, compared to 2.84 Å, the sum of Shannon crystal radii of eight-coordinate Ba^{2+} (1.56 Å) and O^{2-} (1.28 Å).[20]

Final Remarks

We report here the first example of salt-inclusion solids showing the stuctural directing effect due to the nonbonding electrons of the chlorine-centered secondary building unit

(20) Shannon, R. D. *Acta Crystallogr.* **1976**, *A32*, 751−767.

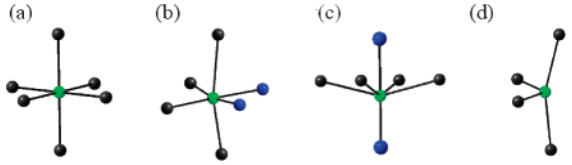

Figure 8. Coordination surrounding chlorine in (a) NaCl, (b) CU-9 and CU-11, (c) CU-13, and (d) CU-14. The electropositive cations are drawn in black, and transition metal cations, in blue.

(SBU). It has been reported that acentric structures can be constructed by incorporating ligands such as selenite or iodate polyanions with nonbonding electron pairs.[21] Some recent research reports also noted the "polar-templating" effects of monatomic halide anions (F^-, Cl^-).[22] In our previouse studies, we illustrated the occurrence of the chlorine-centered $ClA_{6-n}M_n$ acentric SBU by means of the so-called cation substitutions of the otherwise centric $ClNa_6$ unit (Figure 8a). For example, the acentric SBU can occur by dication substitution ($n = 2$) in either the cis positions (Figure 8b), as seen in the CU-9 and CU-11 structures (A = Cs, M = Cu),[7g] or in the trans (Figure 8c) with incorporating the Jahn−Teller Mn^{3+} cation, as shown in CU-13 (A = Ba; M = Mn).[7i] Our present results reveal a new scheme of acentric SBU of the seesaw-shaped $ClBa_4$ (Figure 8d), which adopts a distorted tetrahedral coordination commonly seen in the cubic and hexagonal forms of the bulk $BaCl_2$ structure.[23] In this configuration, the chloride anions of the salt lattice oriented themselves relative to the oxide anions of the covalent framework to minimize the otherwise electron−electron repulsion interaction. This nonbonding interaction, thus, "directs" the preferred orientation of the anionic framework.

As in CU-13, employing combined acentric salt units and polar silicate framework, we have successfully isolated a family (CU-14) of novel polar solids $Ba_6Mn_4Si_{12}O_{34}Cl_3$ and $Ba_6Fe_5Si_{11}O_{34}Cl_3$ via salt-inclusion method. Similar to the synthesis of organic−inorganic hybrid materials, the salt-inclusion route facilitates a promising approach for the directed synthesis of special framework solids, including NCS compounds, via composite lattices. We anticipate that, by controlling the stoichiometric ratio of Ba^{2+}/Cl^-, one may manipulate the charge, shape, size, and geometry of covalent networks, thus allowing more fascinating frameworks yet to come.

Acknowledgment. Financial support for this research (Grants DMR-0077321, 0322905) and the purchase of a single-crystal X-ray diffractometer (Grant CHE-9808165) from the National Science Foundation (NSF) is gratefully acknowledged. The authors are in debt to Dr. G. J. Miller and Mr. J. W. Anderegg of Iowa State University for their assistance with the XPS measurement, Dr. P. S. Halasyamani for the SHG measurement, and Ms. B. J. Ramirez and W. Queen for manuscript preparation. E.F. especially acknowledges the generous financial support provided via the NSF Summer Research Program in Solid State and Materials Chemistry (Grant DMR-0303450).

Supporting Information Available: An X-ray crystallographic file, in CIF format, and complete XPS spectra. This material is available free of charge via the Internet at http://pubs.acs.org.

IC050228T

(21) (a) Bauer, E. M.; Bellitto, C.; Colapietro, M.; Portalone, G.; Righini, G. *Inorg. Chem.* **2003**, *42*, 6345−6351. (b) Ok, K. M.; Halasyamani, P. S. *Inorg. Chem.* **2002**, *41*, 3805−3807. (c) Kwon, Y.-U.; Lee, K.-S.; Kim, Y. H. *Inorg. Chem.* **1996**, *35*, 1161−1167. (d) Harrison, W. T. A.; Dussack, L. L.; Jacobson, A. J. *J. Solid State Chem.* **1996**, *125*, 234−242.

(22) (a) Groves, J. A.; Wright, P. A.; Lightfoot, P. *Inorg. Chem*. **2005**, *44*, 1736−1739. (b) Bull, I.; Villaescusa, L. A.; Teat, S. J.; Camblor, M. A.; Wright, P. A.; Lightfoot, P.; Morris, R. E. *J. Am. Chem. Soc.* **2000**, *122*, 7128−7129.

(23) Haase, A.; Brauer, G. *Z. Anorg. Allg. Chem.* **1978**, *441*, 181−195.